Quantitative phase microscopy of biological samples using a portable interferometer

Natan T. Shaked

Department of Biomedical Engineering, Faculty of Engineering, Tel Aviv University, Tel Aviv 69978, Israel (nshaked@tau.ac.il)

Received January 19, 2012; revised March 21, 2012; accepted March 24, 2012; posted March 27, 2012 (Doc. ID 161779); published May 30, 2012

This Letter presents the τ interferometer, a portable and inexpensive device for obtaining spatial interferograms of microscopic biological samples without the strict stability and the highly coherent illumination that are usually required for interferometric microscopy setups. The device is built using off-the-shelf optical elements and can easily operate with low-coherence illumination, while being positioned in the output of a conventional inverted microscope. The interferograms are processed into the quantitative amplitude and phase profiles of the sample. Based on the phase profile, the optical-path-delay profile is obtained with temporal stability of 0.18 nm and spatial stability of 0.42 nm. Further experimental demonstration of using the τ interferometer for imaging the quantitative thickness profile of a live red blood cell is provided.

OCIS codes: 090.1995, 090.2880, 170.3880, 180.3170.

Interferometric microscopy can be used to simultaneously record the quantitative spatial profiles of both the amplitude and the phase of mostly transparent biological samples. Using interferometric microscopy, time recording of the phase profile can yield remarkable optical thickness or optical-path-delay stability of less than a nanometer, with acquisition rates of several thousands of full frames per second, and without the need for using contrast agents such as fluorescence dyes. Since the technique provides the optical thickness per each spatial point on the sample, various biologically relevant morphological and mechanical parameters can be obtained in a noncontact, label-free manner [1–3].

These unique advantages could be attractive for many clinical applications. However, at this point, there are not many options for commercial interferometric microscopes compared to other microscopy techniques, and this tool is mostly used by optical and biomedical engineers for research purposes. One reason for this is the difficulty of obtaining high-quality and stable interference patterns with modest and portable equipment and without the need for an expert user.

The interference pattern, superimposing the light that has interacted with the sample and a reference beam that comes directly from the source, captures the quantitative amplitude and phase profiles of the sample. The commonly used interferometric setups are usually constructed in open and custom-built microscopes and operated by a user with knowledge in optics. To ensure the stability of the interference pattern, the entire system is positioned on an optical table to avoid mechanical vibrations and is boxed inside an enclosure to avoid differential air perturbations between the interferometric arms.

This situation may be changed in the near future with the introduction of portable and inexpensive wavefront sensing setups that do not necessitate careful alignment of the system before each experiment [4–13]. Furthermore, the fact that many of these new setups operate in common-path interferometric geometry (in which both the sample and the reference beams mostly propagate together) significantly increases the stability of the system and, in some cases, even eliminates the need of positioning the system on an optical table.

One of these setups is the interferometric chamber (InCh) microscope [4]. In this system, all the interferometric elements are encapsulated into a single, rigid, and factory-designed reflective chamber. Although this system uses common-path geometry (and thus can operate without an optical table), it can still create off-axis interferograms of the sample (and thus only one frame is required for acquiring the amplitude and the phase profiles of the sample, which is suitable for highly dynamic samples). However, the InCh microscope cannot use high magnifications due to the fact that the microscope objective also needs to collect the tilted reference beam. In addition, this microscope requires highly coherent illumination sources since the optical-path difference between the reference and the sample beams is twice the optical thickness of the chamber.

Other setups for common-path or self-interference quantitative phase microscopy have been presented lately by Popescu *et al.* [5,6], Jang *et al.* [7], Kemper *et al.* [8], Coppola *et al.* [9], Mico *et al.* [10], and Bon *et al.* [11]. In the first type of setups [5,6,10,11], a diffraction grating or other specialized optical elements are used, whereas in the second type of setups [7,8], a Michelson interferometer in the output of a microscope (or similar digital processing [9]) is used, so that the sample beam interferes with itself, with the limitation that half of the sample is empty.

This Letter proposes the τ interferometer, a new portable and high-accuracy interferometric setup that combines the advantages of both types of methods described above and eliminates part of their disadvantages.

Figure 1 presents an inverted microscope composed of a microscope objective (MO) and a tube lens (L_0) that are positioned in $4f$ configuration [2]. In the output of the interferometer, instead of porting a digital camera, the τ interferometer is positioned. This interferometer receives the magnified image of the sample from the inverted microscope and Fourier transforms it by lens L_1, while splitting it into two beams by the cube beam splitter (BS). A pinhole, placed in the Fourier plane of

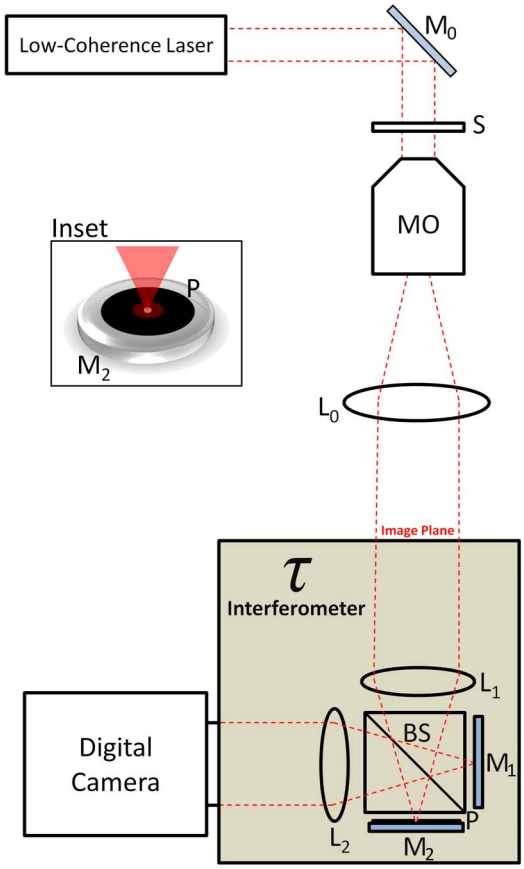

Fig. 1. (Color online) The τ interferometer ported into the output of an inverted microscope. The interference is created by splitting the magnified image from the inverted microscope and effectively erasing the information from one of the beams before combining the beams again. S, sample; MO, microscope objective; L_0, L_1, L_2, spherical lenses; BS, beam splitter; M_0, M_1, M_2, mirrors; P, pinhole (confocally positioned). Inset: expanded figure for the reference-beam mirror M_2.

one of the interferometric arms, effectively erases the sample information by only passing the zero spatial frequencies of the image Fourier transform, which creates a reference beam. The two beams are then reflected by mirrors and combined by the beam splitter. Another lens (L_2), positioned in $4f$ configuration with the first lens (L_1), back Fourier transforms the two beams and projects them onto the camera, where an interferogram of the sample is created, while capturing both the amplitude and the phase profiles of the sample. The setup provides an on-axis interferometric microscope, and an electric control connected to one of the mirrors can create several phase-shifted interferograms that are needed to retrieve the quantitative phase profile of the sample. However, to enable single-exposure operation, off-axis interferograms can be acquired by shifting the mirrors or the camera to high-spatial-frequency region, within the source coherence length as defined later.

Note that only simple optical elements and no gratings or other diffractive elements are used inside the interferometric system, in contrast to the setups proposed in [5,6,10,11]. In addition, there is no limitation on the confluence of the sample (thus, we do not need to use a half-empty sample), in contrast to the setups proposed in [7–9].

Since the sample beam only splits in the end of the system, the proposed setup can be considered as a common-path interferometer, and its stability will be significantly higher compared to regular interferometers. In addition, in contrast to [5,6], in which the reference and the sample beams pass through different locations in free space as soon as they are split by a grating, the sample and the reference beams in our case mostly pass through the glass of the cube beam splitter, and thus there are fewer differential air perturbations between the interferometric arms, even if the interferometer is not boxed. Moreover, since splitting the beam is done inside the $4f$ system, the τ interferometer is closer to the common path than the configurations proposed in [5,6], in which the splitting is done in the beginning of the $4f$ system.

In the τ interferometer, the mirrors are placed right in the outputs of the beam splitter, and since the beams are tightly focused on each of the mirrors (in contrast to [7,8]), it is significantly easier to match the beam paths, and thus it is possible to obtain interference with low-coherence sources.

To demonstrate using the τ interferometer, the system shown in Fig. 1 was constructed. A temporally low-coherence plane wave was created by passing a supercontinuum fiber-laser light (from SC400-4, Fianium) through a computer-controlled acousto-optical tunable filter (SC-AOTF, Fianium), selecting a central wavelength of 633 nm with a full-width-at-half-maximum bandwidth of 6.6 nm, as measured by a compact spectrometer (USB4000, Ocean Optics), coinciding with coherence length of $l_c = 26.8$ μm. The light was collimated using relay optics and input into the inverted microscope. Alternatively, a highly coherent source [633 nm, helium–neon (He–Ne) laser] was used in the input of the inverted microscope.

In the inverted microscope, a 40×, 0.66 numerical-aperture microscope objective and a 15 cm focal-length tube lens (L_0 in Fig. 1) are used. The τ interferometer, ported in the output of the inverted microscope, contained two 7.5 cm focal-length lenses, positioned in $4f$ configuration (L_1 and L_2 in Fig. 1), a cube beam splitter, and two mirrors, with a pinhole of 20 μm positioned in front of one of them. The mirrors were positioned very close to the output of the beam splitter, so that there was almost no propagation through free space after splitting the beams and before combining them. No enclosure was used to avoid differential air perturbations between the interferometric arms, which makes the sample stage and the entire setup more accessible. A monochrome digital camera (DCC1545M, Thorlabs) with square pixels of $\delta = 5.2$ μm was positioned in the output of the τ interferometer to acquire the interferograms of the sample. Within the coherence length of the source and an off-axis angle of 1°, the effective number of pixels, across which interference is obtained, is $2l_c/[\delta \times \mathrm{tg}(1°)] = 590$ pixels, coinciding with a field of view of more than 80 μm on the sample, which is enough for acquiring several cells together. Reference [14] shows that tilting the field of one of the beams can yield high-frequency interference on the entire camera plane.

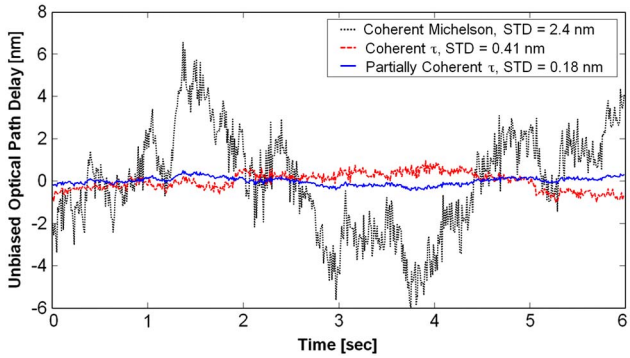

Fig. 2. (Color online) Temporal stability of the optical-path delay of a diffraction-limited spot for a Michelson interferometer using a highly coherent source (dotted curve), τ interferometer using a highly coherent source (dashed curve), and τ interferometer using a partially coherent source (solid curve).

We acquired 100 interferograms per second and processed them into the phase profile of the sample by using a digital spatial filtering of a cross-correlation term from the other terms [1], followed by subtraction of the phase profile obtained from an interferogram without the presence of the specimen, which compensates for phase aberrations introduced by the system, and a phase unwrapping algorithm for removing 2π ambiguities [15].

The dashed curve in Fig. 2 represents the temporal optical-path delay that was obtained using the τ interferometer and the highly coherent He–Ne laser for a representative diffraction-limited spot (approximately 4×4 pixels), with standard deviation of 0.41 nm. For comparison, the dotted curve in Fig. 2 represents the temporal optical-path delay that was obtained using the He–Ne laser in the input of a conventional Michelson interferometer under the same conditions (without using an enclosure) for a representative diffraction-limited spot, with a standard deviation of 2.4 nm. As shown by the solid curve in Fig. 2, when using the low-coherence source while measured in the maximum interference area, the τ interferometer yielded temporal optical-path delay with standard deviation of 0.18 nm.

Under low-coherence illumination, the spatial background noise of 100×100 diffraction-limited spots on a single image has a standard deviation of 0.42 nm, whereas a Michelson interferometer using the He–Ne laser yielded a spatial standard deviation of 3.8 nm, mostly due to the presence of speckle noise.

Figure 3 shows the thickness profile of a human red blood cell obtained by single exposure using the τ interferometer and the low-coherence source. To obtain this thickness profile, we divided the optical-path-delay profile of the cell by the difference between the refractive index of the cell ($n = 1.395$), under the assumption of homogenous refractive index for an enucleated red blood cell [3,5], and the refractive index of the surrounding media ($n = 1.34$). As shown in Fig. 3, due to the use with a low-coherence source, the background around the red blood cell (containing only cell media) is remarkably flat, with a standard deviation of spatially averaged optical-path delay of 0.85 nm in liquid environment.

In conclusion, we have presented the τ interferometer, a compact, portable, and extremely stable interferometric setup that enables recording the amplitude and the phase profiles of biological samples using a low coherence source, without the need for special optical elements and an expert alignment prior to every experiment.

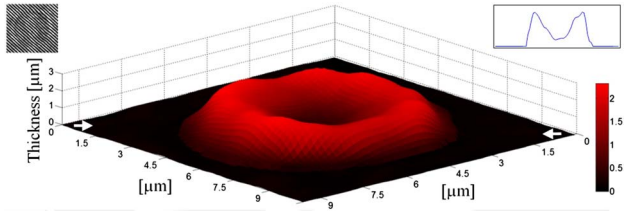

Fig. 3. (Color online) Quantitative thickness profile of a red blood cell acquired with the τ interferometer in a single camera exposure. Color bar represents thickness in μm. Left inset: interferogram of the cell. Right inset: cross section across the diagonal of the phase profile of the cell.

We expect that in mass production, the cost of the τ interferometer will be as low as a couple of hundred dollars (cost of two mirrors, two lenses, a pinhole, a beam splitter, and a cage) and double that if a modulator is used for acquiring phase-shifted on-axis interferograms, with a total size that can be as low as 1 in. (2.54 cm) across. We believe that the fact that this interferometer can be ported in the output of an inverted microscope and operated in a simple way, while still obtaining remarkably high accuracy, will make interferometric phase microscopy more accessible and affordable for biologists and clinicians, while significantly broadening its range of applications.

References

1. N. T. Shaked, J. D. Finan, F. Guilak, and A. Wax, J. Biomed. Opt. **15**, 010505 (2010).
2. N. T. Shaked, L. L. Satterwhite, N. Bursac, and A. Wax, Biomed. Opt. Express **1**, 706 (2010).
3. N. T. Shaked, L. L. Satterwhite, G. A. Truskey, M. J. Telen, and A. Wax, J. Biomed. Opt. **16**, 030506 (2011).
4. N. T. Shaked, Y. Zhu, N. Badie, N. Bursac, and A. Wax, J. Biomed. Opt. **15**, 030503 (2010).
5. G. Popescu, T. Ikeda, R. R. Dasari, and M. S. Feld, Opt. Lett. **31**, 775 (2006).
6. H. Ding and G. Popescu, Opt. Express **18**, 1569 (2010).
7. J. Jang, C. Y. Bae, J.-K. Park, and J. C. Ye, Opt. Lett. **35**, 514 (2010).
8. B. Kemper, A. Vollmer, C. E. Rommel, J. Schnekenburger, and G. von Bally, J. Biomed. Opt. **16**, 026014 (2011).
9. G. Coppola, G. Di Caprio, M. Gioffré, R. Puglisi, D. Balduzzi, A. Galli, L. Miccio, M. Paturzo, S. Grilli, A. Finizio, and P. Ferraro, Opt. Lett. **35**, 3390 (2010).
10. V. Mico, Z. Zalevsky, and J. Garcia, Opt. Commun. **281**, 4273 (2008).
11. P. Bon, G. Maucort, B. Wattellier, and S. Monneret, Opt. Express **17**, 13080 (2009).
12. X. Cui, J. Ren, G. Tearney, and C. Yang, Opt. Express **18**, 16685 (2010).
13. M. Lee, O. Yaglidere, and A. Ozcan, Biomed. Opt. Express **2**, 2721 (2011).
14. Z. Monemhaghdoust, F. Montfort, Y. Emery, C. Depeursinge, and C. Moser, Opt. Express **19**, 24005 (2011).
15. T. Colomb, J. Kühn, F. Charrière, C. Depeursinge, P. Marquet, and N. Aspert, Opt. Express **14**, 4300 (2006).